Online Monitoring of Composition, Sequence Length, and Molecular Weight Distributions during Free Radical Copolymerization, and Subsequent Determination of Reactivity Ratios

H. Çatalgil-Giz,‡ A. Giz,‡ A. M. Alb,† A. Öncül Koç,§ and W. F. Reed*,†

Department of Physics, Tulane University, New Orleans, Louisiana 70118; Faculty of Sciences, Istanbul Technical University, 80626 Maslak, Istanbul, Turkey; and Bahçeşehir University, 34900 Bahçeşehir, Istanbul, Turkey

Received February 6, 2002; Revised Manuscript Received May 16, 2002

ABSTRACT: Exploiting differences in refractivity and ultraviolet absorption between pairs of monomers and their associated polymers, automatic, continuous, online monitoring of polymerization reactions (ACOMP) was extended to copolymerization. ACOMP uses no chromatographic separation columns. Copolymerization of methyl methacrylate and styrene was chosen for developing the method. Both the instantaneous concentrations of comonomers and their incorporation rates into copolymer are obtained, which allows model-independent evolution of the average copolymer composition to be followed. Using the compositional information and simultaneous light-scattering data permits monitoring model-independent M_w (cumulative weight-average molecular weight), without requiring measurements in different solvents. Simultaneous use of a viscometer allows a cross check on the light-scattering data. Molecular weight and composition data are used to obtain the copolymer bivariate mass and composition distribution. Monomer reactivity ratios are found by an errors in variables method. The reactivity ratios and composition distribution allow sequence length distributions to be computed.

Introduction

There is an extensive literature on theoretical, experimental, and applied aspects of copolymerization reactions. Early work on kinetic models includes reports by Mayo and Lewis[1] and Alfrey and Goldfinger.[2] It has long been recognized that the overall composition of the resulting copolymer depends on the ratios of the propagation rate constants known as the reactivity ratios. Other important copolymer characteristics include molecular weight, composition, and sequence length distributions.

The so-called bivariate distribution, in terms of copolymer composition and mass, was first treated theoretically in the 1940s[1−5] and has since been revisited for systems containing multiple comonomers.[6] To determine the bivariate composition and mass distributions from an existing polymer usually requires an involved process of cross-fractionation. Techniques used to determine molar mass and/or composition distributions include HPLC,[7] thermal field-flow fractionation,[8] temperature rising elution fractionation (TREF),[9−11] Fourier transform infrared spectroscopy (FTIR),[12] and other types of elution gradient chromatography[13,14] for determining chemical composition, and size exclusion chromatography (SEC) and related techniques for mass distribution determination,[15,16] including combinations of the above into integrated instruments.[17] Furthermore, the sequence length distribution of a copolymer and associated averages are often important in determining the "blockiness" of the copolymer, microscopic morphology,[18] and macroscopic properties, including solubility, blending and other thermodynamic behavior.[19−22] Knowledge of the reactivity ratios and feed composition is often used to compute sequence length distributions on theoretical grounds.[23] Sequence lengths have also been determined by dynamic scanning calorimetry[24] and NMR,[25,26] as well as chemical degradation of the copolymer and a subsequent analytical technique, such as gel permeation chromatography (GPC).[27−30]

The goal of this work is to extend a recently introduced technique for automatic, continuous, online monitoring of polymerization reactions (ACOMP) to the simultaneous, model-independent determination of the average composition, and mass distributions during free radical copolymerization reactions. Reactivity ratios can be computed as well as model-dependent sequence length distributions. To accomplish this, the differences in differential refractive index and ultraviolet absorption of comonomers A and B, in their monomeric and polymeric forms, are exploited to obtain the monomer and polymer composition as a function of time and, simultaneously, total monomer conversion. With this compositional information it is possible to develop a method for the meaningful analysis of light-scattering data, to determine the absolute weight-average mass M_w as a function of conversion, and hence also to determine the average M_w distribution.

ACOMP methods have been previously introduced and described.[31] They have been extended to include continuous reactors,[32] and have been applied to the detailed determination of acrylamide polymerization kinetics,[33] chain transfer constants,[34] monitoring of polydispersity evolution,[35] and controlled radical polymerization.[36] The aim of ACOMP is 3-fold: (1) to provide polymer scientists with a tool to study fundamental aspects of kinetics and mechanisms in new polymer synthesis, (2) to provide the means for optimizing reactions at the bench and pilot plant levels, and (3) to ultimately allow online monitoring and control of polymer production at the full industrial scale reactor level. A further benefit in the latter case is that, in

* Correspondence author.
† Tulane University.
‡ Istanbul Technical University.
§ Bahçeşehir University.

10.1021/ma0201983 CCC: $22.00
Published on Web 07/19/2002

Table 1. Monomer, Solvent, and Polymer Characteristics[a]

	$\partial n/\partial c_p$ in Bu−Ac at p_f (Table 2)	monomer mass (g/mol)	density (g/cm^3)	A_2	$[\eta]$ (cm^3/g)	expt no.
Sty	0.162	104.15	0.909	xx[c]	xx	
MMA	0.019	100.12	0.936	xx	xx	
butyl acetate[b]	xx	xx	0.882	xx	xx	
AIBN	0.043		xx	xx	xx	
Sty, 100%	0.203	xx	1.04	0.00045	7.3	VI
Sty/MMA 3/1	0.166	xx	xx	0.00046	7.6	V
Sty/MMA 1/1	0.149	xx	xx	0.00045	9	IV
Sty/MMA 1/3	0.128	xx	xx	0.00027	9.4	III
Sty/MMA 1/9	0.114	xx	xx	0.00013	10.0	II
MMA 100%	0.099	xx	1.18	0.00013	8.4	I

[a] Also shown is the list of experiments according to the ratio (g/g) of Sty/MMA. All experiments were at 65 °C, with 2.4% by mass of AIBN for initiation. ACOMP mixing was, by volume, 8% from the reactor and 92% from the BuAc solvent reservoir, with a total flow rate through the detector train of 2 mL/min [b] $n = 1.3940$. [c] xx = not applicable, not definable, or not relevant to the present analysis.

addition to helping control properties of the copolymer during the reaction, the final product emerges well characterized.

Experimental Section

ACOMP Instrumentation. The ACOMP technique itself has been adequately described but is undergoing constant improvement. Briefly, a small amount of reactor material is continuously removed from the reactor and mixed with a much larger volume of pure solvent. The continuously diluted polymer solution passes through a train of detectors comprising a home-built multiangle light-scattering chamber,[37] a home-built single capillary viscometer,[38] a Shimadzu SPD-10AV ultraviolet spectrophotometer (UV), and a Waters 2410 differential refractometer (RI). No chromatographic columns are used, and no injections of discrete amounts of sample are made; i.e., this is not a flow injection method.

Significant modification of the automatic continuous dilution process was developed for this work, where it was necessary to ensure that the pump extracting from the reactor maintained a precisely known flow rate and that the abundant bubbles produced during the reaction did not enter the pump, since this would cause it to send a gas-laden sample stream to the detectors, destroying their monitoring capabilities. The problem of maintaining a precise volume withdrawal rate was solved by using two Hewlett-Packard 1100 isocratic pumps and attaching their outputs to a high-pressure micromixing chamber. The constant flow rate of the pump withdrawing from the reactor is maintained at the expense of increasing backpressure as the reaction liquid becomes more viscous as conversion proceeds. The problem of bubbles was solved by interposing an ISCO gradient programmer between the reactor and the input of the isocratic pump withdrawing from it. The mixing chamber of the gradient programmer has a debubbling feature, which allows all bubbles entering the chamber to be exhaled through the purge outlet. Still, because of the increase of viscosity of the reactor solution as polymerization proceeds, there came a point in each reaction in which either the pump pressure exceeded a preset safety level of 50 bar or cavitation caused the reactor-side pump to deprime. Hence, 100% conversion was not achieved in the reactions but typically ranged from 50% to 75%. Meanwhile, efforts are underway to develop a more robust automatic extraction/dilution system that will be effective to much higher reactor viscosities.

Data gathering and analysis software was written by the authors. The response time of the system, due to mixing effects was determined to be about 200 s, which means that reactions going to complete conversion on this time scale are at the limit of resolution. Since this response time is just a function of "plumbing", it can be reduced much further by appropriate design, if desired.

Monomer Preparation and Polymerization Reactions. Methyl methacrylate (MMA) and styrene (Sty), both from Aldrich, were freed from inhibitor by washing with 5% sodium hydroxide solution two times and then with water several times, until the water had a neutral pH. Monomers were dried over calcium sulfate and fractionally distilled and stored at 4 °C. Initiator, azobisizobutyronitrile (AIBN), and the carrier solvent butyl acetate (BuAc) were used as received (Aldrich).

Before beginning the polymerization reaction, pure BuAc was pumped through the detector train to obtain the baseline of each instrument. After stabilization, Sty, in the desired initial concentration, was pumped at a flow rate of 0.16 mL/min from the reactor and continuously diluted with a flow of 1.84 mL/min of BuAc from the solvent reservoir. These same flow rates from the reactor and reservoir were maintained throughout the entire experiment. The diluted solution always reached the detector train at $T = 25$ °C, regardless of the reactor temperature. The Sty stabilization step was taken to ensure good UV detector calibration for the starting concentration of Sty. The reaction vessel, containing a total of 25% total monomer and 75% BuAc by mass, with a total reaction liquid mass of about 150 g, which had been previously purged for 15 min with N_2, was then lowered into a temperature-controlled bath at 65 °C. ACOMP withdrawal and dilution continued at the fixed ratio stated, and the reaction mixture was allowed to flow until stabilization of the detectors occurred.

The reactions were initiated by adding AIBN in powder form. The solution was magnetically stirred during the reaction. The reactor temperature was monitored with a thermocouple whose signal was integrated into the data acquisition software. Conversion of monomer to polymer was followed with the decrease of UV absorption of the monomer during polymerization reactions at 282 nm and with RI measurements. The value of $\partial n/\partial c$ (differential refractive index increment) of monomers, polymers, and initiator are given in Table 1, along with the labeling scheme for the various experiments, which were carried out at varying initial mass ratios of Sty and MMA. The differential refractive indices of poly(methyl methacrylate) (PMMA) and polystyrene (PS) were determined during ACOMP measurements of homopolymerization reactions according to the method recently developed by Brousseau et al.[39]

As mentioned above, reactions were terminated when the pump pressure reached a preset limit, or if the reactor draw pump deprimed. The contents of the reactor were added to methanol immediately after termination, and the polymer was precipitated for subsequent GPC and other measurements.

Determination of Comonomer and Polymer Concentrations from ACOMP. The concentrations of the two comonomers in their monomeric form must be computed from the raw RI and UV data, as well as the concentrations of each incorporated into polymer. In this work c_A refers to the mass concentration of species A in g/cm^3, whereas [A] is the molar concentration. Throughout this work Sty will be taken as monomer A and MMA as B. The UV voltage V_{UV} at a specific wavelength is composed of the signals from each of the four species:

$$V_{UV} = s\left(\frac{\partial V_{UV}}{\partial c_{mA}}c_{mA} + \frac{\partial V_{UV}}{\partial c_{pA}}c_{pA} + \frac{\partial V_{UV}}{\partial c_{mB}}c_{mB} + \frac{\partial V_{UV}}{\partial c_{pB}}c_{pB}\right) \quad (1)$$

where c_{mA} and c_{pA} are the monomer and polymer concentrations in the reactor of species A, and likewise for c_{mB} and c_{pB}, and s is the fraction of the volume flow to the detector train coming from the reactor. Throughout this work $s = 0.08$. In principle, all four species could each have useful and distinct UV absorption spectra, so that four equations could be generated by monitoring four separate wavelengths, which would fully determine the system, without additional signals or use of mass conservation equations. In this work, however, only styrene has significant UV absorption, so that at least one more data signal that yields an additional equation, coupled with two mass conservation equations, is needed.

The second signal comes from the RI. The refractive index detector voltage V_{RI} is given by

$$V_{RI} = s\left(\frac{\partial n}{\partial c_{mA}}c_{mA} + \frac{\partial n}{\partial c_{pA}}c_{pA} + \frac{\partial n}{\partial c_{mB}}c_{mB} + \frac{\partial n}{\partial c_{pB}}c_{pB}\right)\frac{dV}{dn} \quad (2)$$

where dV/dn is the calibration factor of the RI: i.e., the RI voltage output per index of refraction unit. Here, it is assumed that the refractivity of the solution is simply the sum of the refractivities of the component monomers and corresponding homopolymers. The summation of refractivities of the monomers in dilute solution should be nearly exact, whereas the assumption that the refractivity of a copolymer of given composition is the same as that of a mixture of homopolymers of the same concentration composition of A and B is less obvious. This approximation has been used extensively, however, since the first treatments of light scattering by copolymers were made[40,41] and has been borne out through the years by experimental measurements.

Using conservation of mass of A and B in the reactor, together with the density differences existing among the monomers, polymers and solvent, allows the volume of fluid in the reactor to be expressed, ideally, as

$$V_{reactor} = V_{solvent}(1 + R_A + R_B - \delta_A R_A p_A - \delta_B R_B p_B) \quad (3)$$

and conversion of monomer A, p_A, as

$$p_A = \frac{1 - \dfrac{c_{mA}(1 + R_A + R_B - \delta_B R_B p_B)}{c_{mA,0}(1 + R_A + R_B)}}{1 - \dfrac{c_{mA}\delta_A R_A}{c_{mA,0}(1 + R_A + R_B)}} \quad (4)$$

where p_B is the conversion of monomer B, R_A is the initial volume of monomer A to solvent volume, and likewise for R_B, $c_{mA,0}$ is the initial concentration of monomer A, and

$$\delta_A = 1 - \frac{\rho_{mA}}{\rho_{pA}} \quad (5)$$

where ρ_{mA} and ρ_{pA} are the densities of monomer A and homopolymer A, respectively. Ideality of mixing is assumed in these derivations. p_B is obtained by simply interchanging subscripts A and B in each equation.

In the absence of density corrections p_A recovers the more familiar form

$$p_A = 1 - \frac{c_{mA}}{c_{mA,0}} \quad (6)$$

The relationship between the polymer concentration and conversion is determined through conservation of mass to be

$$c_{pA} = \frac{p_A m_{A,0}}{V_S(1 + R_A + R_B - \delta_A R_A p_A - \delta_B R_B p_B)} \quad (7)$$

where $m_{A,0}$ is the initial mass of monomer A in the solvent volume V_S.

Hence, analysis of the RI and UV data according to the above scheme yields a continuous record of the monomer concentrations $c_{mA}(t)$ and $c_{mB}(t)$, as well as the concentration of A and B involved in copolymer $c_{pA}(t)$ and $c_{pB}(t)$. Knowledge of these concentrations yields extraordinary analytical power for characterizing instantaneous average and integrated average properties of the copolymer, while it is being produced.

Most of the expressions involving concentrations in this work involve ratios, in which case the concentrations in the reactor and detector train can be used interchangeably, since the dilution factor, s, will cancel in the numerator and denominator. Concentrations in the detector train must be used, however, when interpreting the detector signals. In those cases, an explicit statement will be made.

Viscosity Determination. The viscometer was a single capillary mounted via T-connectors to a Validyne Engineering differential pressure transducer, and has been discussed in detail.[38] Total solution viscosity is

$$\eta = \eta_s[1 + [\eta]c_p + k_p[\eta]^2 c_p^{\,2}] \quad (8)$$

where η_s is the pure solvent viscosity, $[\eta]$ is the intrinsic viscosity of the polymer, c_p is here the total copolymer concentration in the detector, and k_p is a constant related to the hydrodynamic interactions between polymer chains, usually around 0.4 for neutral, coil polymers.[42] The intrinsic viscosity is the extrapolation to zero concentration and zero shear rate of the reduced viscosity η_r.

Size Exclusion Chromatography (SEC). Results of terminal M_w and $[\eta]$ from ACOMP were compared with SEC results, both because SEC continues to be the analytical method of choice for many polymer scientists determining M_w, and because SEC gives a complete mass distribution. The SEC system used an Agilent 1100 isocratic pump, Polymer Laboratories PL gel 10 mixed B columns, an Anspec refractometer, a home-built single capillary viscometer previously described in detail, and a home-built light-scattering instrument identical to the one used for the ACOMP measurements. This instrument has been described previously,[37] and its use for SEC has been demonstrated.[43] The light-scattering analysis is different than that used for homopolymers, and this is discussed below.

Determination of Reactivity Ratios, Composition, Mass, and Sequence Length Distributions from ACOMP

In the simplest paradigm for propagation in free radical reactions, it is assumed that the rate of reaction for a given comonomer depends only on which monomer bears the radical at the chain terminus. For the molar concentrations of monomer [A] and [B], this leads to propagation equations of the form

$$-\frac{d[A]}{dt} = k_{AA}[A][A^*] + k_{BA}[A][B^*] \quad (9a)$$

$$-\frac{d[B]}{dt} = k_{BB}[B][B^*] + k_{AB}[B][A^*] \quad (9b)$$

where A* and B* are the propagating radicals of A and B, respectively. The quasi steady-state approximation assumes that the rate at which [A*] and [B*] change is low compared to the other rates in the reaction ($d[A^*]/dt \approx 0$, and similarly for B*). The instantaneous composition of copolymer is then the Mayo−Lewis copolymer equation[1]

$$\frac{d[A]}{d[B]} = \left(\frac{[A]}{[B]}\right)\left(\frac{r_A[A] + [B]}{[A] + r_B[B]}\right) \quad (10)$$

where the reactivity ratios r_A and r_B are defined as

$$r_A = \frac{k_{AA}}{k_{AB}}, \quad r_B = \frac{k_{BB}}{k_{BA}} \tag{11}$$

The instantaneous mole fraction of [A] incorporated, F_A, is given by

$$F_A \equiv \frac{d[A]}{d[A+B]} = \frac{r_A f_A^2 + f_A(1-f_A)}{r_A f_A^2 + 2f_A(1-f_A) + r_B(1-f_A)^2} \tag{12}$$

where f_A and f_B are the mole fractions of monomer A and B, respectively, at any instant,

$$f_A = \frac{[A]}{[A]+[B]}, \quad f_B = \frac{[B]}{[A]+[B]} \tag{13}$$

F_B is obtained by interchanging the subscripts A and B. These expressions form the basis for finding composition and sequence length distributions.

Reactivity Ratios from the Online Data. Leaving aside the early single point linear methods, contemporary approaches are based on an analytical solution of the copolymerization equation, such as the one given by Mayo,[1] or the Skeist[44] solution. Experimental errors emanate from measurements of initial monomer composition, final polymer composition and the degree of conversion. Many authors have shown that nonlinear methods minimizing χ^2 and taking error propagation and individual errors on each of the measurements into account are superior in error handling.[45−49] They avoid much of the distortion of the error structure that is inherent in the linear methods and have smaller and better defined regions for a given percent probability. In traditional experimental methods, to obtain the parameters r_A and r_B, one needs the ratios of initial monomer concentrations, final monomer concentrations or the concentrations of the two monomers in the polymer, and the conversion ratio. While earlier nonlinear methods could take into account only one of these sources, more recent errors in variables methods (EVM)[50−54] take errors emanating from all three of the measurements into account.

In this work a recent EVM developed especially for on-line monitored reactions and based on a numerical, rather than an analytical solution of the copolymerization equation is used to obtain the reactivity ratios.[55] As the monomer concentrations, c_A and c_B, and therefore [A] and [B] are known throughout the reaction, the evolution of these values are compared with numerical solutions of the copolymerization equation as A and B are depleted. In this method the errors in UV and IR measurements during the reaction and also during the initial plateaus are used to find the variance of [A] in the χ^2 calculations.

$$\chi^2 = \sum_{j=1}^{n(\text{exp})} \sum_{i=1}^{n(\text{data})} ([A]([B]_{ij},[A]_0[B]_0) - [A]_{ij})^2/\text{Var}([A]_{ij}) \tag{14}$$

Here the index "*j*" denotes the experiment number and the index "*i*" the data point of that experiment. The variation $\text{Var}([A]_{ij})$ includes the contributions from fluctuations in the signal and the baseline value as well as the calibration constants of both the UV and RI measurements. The sum runs over all data points in all of the experiments.

Instead of using a minimization procedure, we sweep through the r_A, r_B parameter space to obtain χ^2 as a function of the two reactivity ratios generating a map. Although a χ^2 map can be obtained from a single experiment, for a reliable set of reactivity ratios, three experiments with widely differing initial compositions are used.

Note that while in single point methods the composition drift is a problem to be dealt with, here it is actually made use of. Also, data taken during the whole reaction are used, instead of a single datum at the end of the reaction.

It should be noted that since there are calibration errors as well as random experimental errors, the fluctuation in the signal is not the sole source of the variation of the concentration [A]. When there are sufficiently enough data points without separate variations, it is permissible to use the data itself to obtain the variations.[56]

The Instantaneous Average Composition Distribution. The remaining mass fraction of monomer A at any point is given by *x*

$$x = \frac{c_{mA}}{c_{mA} + c_{mB}} \tag{15}$$

The total mass conversion of monomer is defined as

$$p = 1 - \left(\frac{c_{mA} + c_{mB}}{c_{mA,0} + c_{mB,0}}\right)\left(1 - \frac{\delta_A R_A p_A + \delta_B R_B p_B}{(1 + R_A + R_B)}\right) \tag{16}$$

The instantaneous average value of A incorporated into polymer, in terms of mass, at any instant or degree of conversion is $z(p)$,

$$z(p) = \frac{dc_{mA}(p)}{d(c_{mA}(p) + c_{mB}(p))} \tag{17}$$

p and *z* can be computed from the online values of c_{mA} and c_{mB}, so that a fractional population distribution, $\partial p/\partial z$ can be determined at each point during the reaction. The dependence on the instantaneous weight-average mass, $M_{w,inst}$, is discussed below. It is cautioned that taking derivatives of data with noise usually presents technical challenges if meaningful derivatives are to be found. $(\partial p/\partial z)\, dz$ is the fraction of the copolymer population that has a fractional styrene mass content between *z* and $z + dz$. Its computation requires taking a derivative of *p* with respect to *z*, which is already built on derivatives of the data. Unless the data have exceptionally low noise, it will be more profitable to fit c_{mA} and c_{mB} to functional forms, from which analytical expressions for $\partial p/\partial z$ can be found online. An alternative is to build histogram representations of $\partial p/\partial z$, by building up concentrations in specified intervals of *z*.

Because $\partial p/\partial z$ is built on the average instantaneous values, *z*, there is no knowledge of the width of the instantaneous value. The current methodology does not provide a means of experimentally determining this. Widths, based on theory, can be assumed and convoluted with $\partial p/\partial z$, to provide an approximation to the full bivariate distribution $w(l,u)$, discussed below.

The Sequence Length Distribution (SLD). Whereas the average composition distribution is model independent, use of the Mayo−Lewis theory allows a model-dependent SLD to be computed.

Let W_{AA} be the probability that A* adds to A. Using the reactivity ratios, this can be expressed, at any conversion point p, during the reaction as

$$W_{AA}(p) = \frac{r_A f_A(p)}{f_A(p)(r_A - 1) + 1} \tag{18}$$

The probability of having a sequence of k monomers in a row of type A, followed by a monomer B, $P_{A,k}$, then follows the well-known geometric distribution[57,58]

$$P_{A,k} = (1 - W_{AA}){W_{AA}}^{k-1} \tag{19}$$

$P_{A,k}(p)$ from ACOMP measurements at each point p is hence the instantaneous sequence length distribution. The moments of this distribution are well-known. The instantaneous number-average sequence length of monomer A, $\langle N_A \rangle_n$, at conversion point p, is

$$\langle N_A \rangle_n(p) = \frac{1}{1 - W_{AA}(p)} \tag{20}$$

while the instantaneous weight-average sequence length of A, $\langle N_A \rangle_w$ is

$$\langle N_A \rangle_w(p) = \frac{1 + W_{AA}(p)}{1 - W_{AA}(p)} \tag{21}$$

The cumulative values of the number and weight averages, $\langle N_A \rangle_{n,cumu}$ and $\langle N_A \rangle_{w,cumu}$, can be found by simply summing, or integrating, over all conversion points

$$\langle N_A \rangle_{cumu}(p) = \frac{\int_0^p \langle N_A \rangle (p')\, dp'}{p} \tag{22}$$

where the cumulative averages of any moment (e.g., n or w) is obtained by using the corresponding instantaneous average in the integrand.

To obtain the appropriate expressions for monomer B, the subscript B is substituted for A in each variable in the above equations.

***M*w and Mass Distributions from ACOMP.** Whereas differences in $\partial n/\partial c$ between homopolymers of A and B allow ACOMP to follow the instantaneous compositional changes during copolymerization, this very difference leads to well-known complications in the interpretation of light-scattering data, compared to the straightforward situation when scattering from homopolymers is measured. Stockmayer et al.[40] and Bushuk and Benoit[41] derived relatively simple expressions for interpreting copolymer scattering data.

For homopolymers the Zimm[59] single contact approximation is generally used to determine M_w, the z-average mean square radius of gyration $\langle S^2 \rangle_z$, and the second virial coefficient A_2, via extrapolation to $c_p = 0$ and $q = 0$ of the following expression

$$\frac{K' \nu^2 c_p}{I(q,c_p)} = \frac{1}{M_w}\left(1 + \frac{q^2 \langle S^2 \rangle_z}{3}\right) + 2A_2 c_p + O({c_p}^2) \tag{23}$$

where c_p is the concentration of the homopolymer in the detector and q is the scattering vector with the usual definition

$$q = \frac{4\pi n}{\lambda} \sin(\theta/2) \tag{24}$$

where θ is the angular position of the scattering detector. K' is an optical constant, given for vertically polarized light as

$$K' = \frac{4\pi^2 n^2}{N_A \lambda^4} \tag{25}$$

and

$$\nu = \frac{\partial n}{\partial c_p} \tag{26}$$

For the home-built light-scattering detector used in this work a vertically polarized diode laser of vacuum wavelength 677 nm was used. Absolute excess Rayleigh scattering ratios $I(q,c_p)$—total polymer solution scattering minus solvent scattering—were determined at each angle by the method reported in detail in refs 31, 33, and 37.

For copolymers in the dilute solution limit, it was realized long ago that the intensity of scattered light is not related to M_w as directly as in the homopolymer case. In fact, when the quantity $K'\nu^2/I(q,c_p)$ is extrapolated to $c_p = 0$ and $q = 0$ for a copolymer, whose $\langle S^2 \rangle^{1/2} \ll \lambda$, present in a solution of total copolymer concentration c_p, an apparent molecular weight, M_{ap}, is obtained

$$\frac{1}{M_{ap}} = c_p \xrightarrow[q \to 0]{\lim} 0 \frac{K' \nu^2 c_p}{I(q,c_p)} \tag{27}$$

which is related to the true copolymer M_w as discussed below. M_{ap} is composed of the sum over all the compositional elements constituting the copolymer population,[41] that is, each concentration element i has an assigned pair of values of composition and mass

$$M_{ap} = \frac{1}{\nu^2} \sum \gamma_i {\nu_i}^2 M_i \tag{28}$$

where γ_i is the weight fraction of the polymer population with a given pair of composition and mass values

$$\gamma_i = \frac{c_i}{c_p} \tag{29}$$

and ν is the value of $\partial n/\partial c_p$ measured for the copolymer solution, which is given by

$$\nu = \frac{\partial n}{\partial (c_{pA} + c_{pB})} = y\nu_A + (1 - y)\nu_B \tag{30}$$

and y is the mass fraction of accumulated polymer composed of A

$$y = \frac{c_{pA}}{c_{pA} + c_{pB}} \tag{31}$$

Similarly, ν_i is the incremental refractive index of the sub-population of copolymer of fraction γ_i

$$\nu_i = z_i\nu_A + (1 - z_i)\nu_B \tag{32}$$

where z_i is the mass fraction of copolymer of mass M_i composed of A

$$z_i = \frac{c_{pA,i}}{c_{pA,i} + c_{pB,i}} \tag{33}$$

using these definitions of γ_i, ν_i, and z_i in eq 28 leads to Benoit's expression

$$M_{ap}\nu^2 = \nu_A\nu_B M_w + \nu_A(\nu_A - \nu_B)yM_A + \nu_B(\nu_B - \nu_A)(1 - y)M_B \tag{34}$$

where M_A and M_B are the weight averages of the portion of copolymer constituted by A and B, respectively, that is

$$M_A = \frac{\sum z_i^2 c_{pi} M_i}{yc_p} \tag{35}$$

and

$$M_B = \frac{\sum (1 - z_i)^2 c_{p,i} M_i}{(1 - y)c_p} \tag{36}$$

where $c_{p,i}$ is the concentration of polymers of weight fraction z_i with a mass M_i. M_w has the usual definition

$$M_w = \frac{\sum c_{p,i} M_i}{c_p} \tag{37}$$

To obtain the correct M_w traditionally, for a copolymer of unknown composition, it was hence necessary to perform light-scattering experiments in three different solvents (i.e., three different values each for ν_A and ν_B) to determine the three unknowns M_w, M_A, and M_B. Only in the case of a homogeneous composition distribution is $M_{ap} = M_w$.

Because M_{ap}, c_{pA} and c_{pB} are known at each sampling point i in the online experiments, however, it is possible to obtain the correct value of M_w for the copolymer at each instant of the ACOMP experiment. In fact, Benoit's numbering over the index i lends itself naturally in an ACOMP experiment to finite intervals of conversion, as p goes from 0 to 1; i.e., ACOMP follows the incremental buildup of the final copolymer composition and mass distribution until the reaction is stopped or completed. As pointed out by Benoit,[41] the use of a double sum over both composition and mass in eq 28 is avoided by introducing the single index i, and bearing in mind that for a given composition there can be more than one corresponding mass: if the instantaneous width of the composition distribution is considered and/or if $M_w(p)$ is not monotonic. In this latter case, ACOMP can follow the possible multivalued nature of the function $\gamma_i(M)$, since composition and mass measurements are made simultaneously during the polymerization.

Over each conversion interval, i, in the reaction the new increment to the polymer distribution has its own value of z_i over the interval given by

$$z_i = \frac{\Delta c_{mA,i}}{\Delta c_{mA,i} + \Delta c_{mB,i}} \tag{38}$$

where $\Delta c_{mA,i} = c_{mA,i} - c_{mA,i-1}$, and likewise for $\Delta c_{mB,i}$.

Now, only in the case where z_i is constant—i.e., for a copolymer of homogeneous comonomer composition (ignoring the natural width of the composition distribution)—is there a simple relationship between M_w and M_A and M_B

$$M_w = M_A + M_B \quad \text{(for homogeneous composition only)} \tag{39}$$

Here, we present an approach to finding $M_w(p)$ from the measured values of absolute scattering $I(q,c_p)$ and the continuous knowledge of $c_{mA}(p)$, $c_{mB}(p)$, $c_{pA}(p)$, and $c_{pB}(p)$ afforded by ACOMP. These latter concentrations allow immediate computation of $y(p)$ by eq 31 and $\nu(p)$ by eq 30. To aid in the solution $M_w(p)$, it is advantageous to use a continuous representation of $z(p)$, according to eq 17. If $M_{w,inst}(p)$ is the instantaneous weight-average polymer mass produced in the conversion interval p to $p + dp$ then $M_A(p)$ can be written as

$$M_A(p) = \frac{\int z(p')^2 M_{w,inst}(p')\, dp'}{yp} \tag{40}$$

where $M_{winst}(p)$ is given by[35]

$$M_{w,inst}(p) = \frac{\partial(pM_w)}{\partial p} = M_w(p) + p\frac{\partial M_w}{\partial p} \tag{41}$$

Likewise, $M_B(p)$ is found according to

$$M_B(p) = \frac{\int [1 - z(p')]^2 M_{w,inst}(p')\, dp'}{(1 - y)p} \tag{42}$$

The instantaneous apparent mass, $M_{ap,inst}(p)$, is given by

$$M_{ap,inst}(p) = \frac{\partial(pM_{ap})}{\partial p} = M_{ap}(p) + p\frac{\partial M_{ap}}{\partial p} \tag{43}$$

With these substitutions, eq 34 becomes

$$\nu^2 M_{ap} = aM_w + b\frac{\int z^2 m\, dp'}{p} + c\frac{\int (1 - z)^2 m\, dp'}{p} \tag{44}$$

where for economy of notation

$$a = \nu_A\nu_B \tag{45a}$$

$$b = \nu_A(\nu_A - \nu_B) \tag{45b}$$

$$c = \nu_B(\nu_B - \nu_A) \tag{45c}$$

$$m = M_{w,inst}(p) \tag{45d}$$

$$m_{ap} = M_{ap,inst}(p) \tag{45e}$$

Table 2. ACOMP Results for Monomer Decay Rates, Final Conversion p_f, Final, Cumulative Weight Average Sequence Lengths, Average Final Styrene Composition, M_w, and η_r[a]

							ACOMP			SEC	
expt no.	initial % Sty	$\alpha_{Sty} \times 10^5$ (s^{-1})	$\alpha_{MMA} \times 10^5$ (s^{-1})	p_f	$\langle N_{Sty}\rangle_{w,cum}$:$\langle N_{MMA}\rangle_{w,cum}$	av final Sty comp	$M_{w,fin}$ (kg/mol)	$[\eta]_{fin}$	$M_{w,SEC}$ (kg/mol)	M_w/M_n	M_z/M_w
I	0	xx[b]	7.15	0.65	xx	0.0	32.0	12.4	28.8	1.38	1.28
II	10	11.2	8.10	0.47	1.02:13.33	0.120	19.8	10.2	20.6	1.44	1.30
III	25	5.97	5.00	0.72	1.13:5.21	0.266	12.9	8.7	12.8	1.41	1.31
IV	50	3.08	4.15	0.70	1.54:2.04	0.463	9.1	8.5	9.2	1.52	1.41
V	75	2.27	4.97	0.50	3.47:1.43	0.630	8.3	6.6	8.8	1.37	1.33
VI	100	2.15	xx	0.38	xx	1.0	8.1		8.5	1.53	1.50

[a] The SEC results on the end products are also shown. [b] xx = not applicable, not definable, or not relevant to the present analysis.

and the explicit dependence of each variable on p has been dropped. Multiplying both sides of eq 44 by p and taking the derivative of each side with respect to p yields

$$\frac{\partial(p\nu^2 M_{ap})}{\partial p} = a\frac{\partial(pM_w)}{\partial p} + bz^2 m + c(1-z)^2 m \quad (46)$$

Using eqs 41 and 43 we get

$$\nu^2 m_{ap} + pM_{ap}\frac{d\nu^2}{dp} = m[a + bz^2 + c(1-z)^2] \quad (47)$$

using the integral form of eq 37

$$M_w(p) = \frac{\int m\, dp'}{p} \quad (48)$$

allows $M_w(p)$ to be found by integrating the factored m in eq 47 to yield

$$M_w(p) = \frac{1}{p}\int \frac{\left[\nu^2 m_{ap} + pM_{ap}\frac{d\nu^2}{dp}\right]}{[a + bz^2 + c(1-z)^2]} dp' \quad (49)$$

Operationally, the numerical values of $y(p)$, $z(p)$, $M_{ap}(p)$, and $m_{ap}(p)$, the latter computed from the derivative of $M_{ap}(p)$ according to eq 43, can be inserted into eq 49 and integrated numerically, or forms resulting from fits to $c_{mA}(p)$, $c_{mB}(p)$, and $M_{ap}(p)$ can be inserted.

These computations lead to the important conclusion that, given the ability to monitor the light scattered by a diluted copolymer solution as the copolymer is produced, together with simultaneous measurements of c_{pA} and $c_{p,B}$, the true M_w of the evolving copolymer population can be monitored by ACOMP.

Equation 49 shows that the relationship between $M_{ap}(p)$ and $M_w(p)$ can evolve in a complex fashion. In the special case where $\nu = 0$; i.e., where ν_A and ν_B have opposite signs and y is such that the contributions in eq 30 cancel; M_{ap} can diverge to infinity since, due to a heterogeneous composition, the intensity scattered will not be zero. In the case of low composition drift and like sign values of ν_A and ν_B that do not differ greatly, the correction between M_{ap} and M_w will, in general, be small. This is the case in the current work.

For example, if $c_{mA}(t)$ and $c_{mB}(t)$ follow ideal first-order kinetics (simple exponential decay), then p, y, and z can be parametrized in time. In the limit where density corrections to p are negligible, $p(t)$, $z(t)$, and $y(t)$ are given by

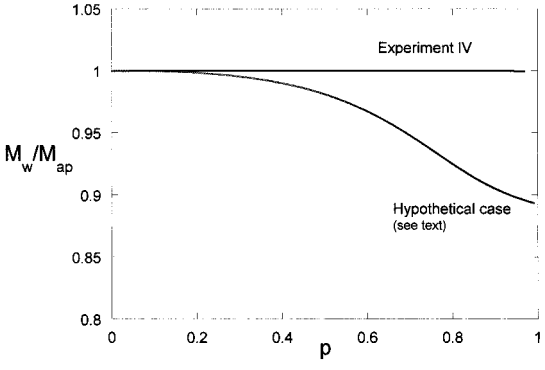

Figure 1. Light-scattering correction factor M_w/M_{ap}, as described in the text. One curve uses the parameters for experiment IV, whereas the other uses related, hypothetical values for the rate constants and initial monomer concentration ratios. In both cases, M_{ap} is taken as constant.

$$p(t) = \frac{c_{mA}(0)[1 - e^{-\alpha_A t}] + c_{mB}(0)[1 - e^{-\alpha_B t}]}{c_{mA}(0) + c_{mB}(0)}, \quad (50)$$

$$y(t) = \frac{1}{1 + \frac{c_{mB}(0)[1 - e^{-\alpha_A t}]}{c_{mA}(0)[1 - e^{-\alpha_B t}]}} \quad (51)$$

and

$$z(t) = \frac{1}{1 + \frac{\alpha_B c_{mB}(0)}{\alpha_A c_{mA}(0)} e^{-(\alpha_B - \alpha_A)t}} \quad (52)$$

In the current work $M_{ap}(p)$ showed little change (see Results), for reasons to be discussed. Taking M_{ap} as constant in eq 49, with eqs 50−52, and using $c_{mA}(0) = c_{mB}(0)$, and α_A, and α_B for experiment IV in Table 2 yields the ratio M_w/M_{ap} shown in Figure 1. The value is virtually unity throughout, reflecting the fact that this experiment and the others were never very far from azeotropy. Also shown in Figure 1 is a hypothetical case where M_{ap} is again constant, $\alpha_A/\alpha_B = 0.2$, and $\nu_A = 0.2$ and $\nu_B = 0.02$. In this case the correction factor changes modestly during conversion.

In the monitoring experiment the scattering, c_{pA}, and $c_{p,B}$ are all determined as functions of time. Furthermore, total monomer conversion, defined in eq 16, can be simultaneously constructed from the measured values of the comonomer concentrations, so that M_w can be given at any instant of monitoring in terms of the time point t_i, or the conversion point p_i. The latter representation allows online approximations to the evolution of polydispersity to be made from a straightforward adaptation of the method recently described.

This allows the fractional mass distribution $\partial p/\partial M_{w,inst}$ at any point to be determined, either by the derivative or histogram methods. $(\partial p/\partial M_{w,inst})dM_{w,inst}$ represents the fraction of the copolymer population with mass between $M_{w,inst}$ and $M_{w,inst} + dM_{w,inst}$. This distribution can also be represented by histogram methods. $p(z,M_{w,inst})$ represents a curve in the space composed of z and $M_{w,inst}$. To convert this into a surface vs z and $M_{w,inst}$ requires assumptions about the instantaneous widths of both z and $M_{w,inst}$. This is considered in the next section.

Model-Dependent Instantaneous and Cumulative Composition and Mass Distributions. The instantaneous average composition and mass distributions treated up to this point are not dependent on any specific models. ACOMP will yield these average distributions based solely on the experimental data.

The instantaneous averages can be fleshed out by invoking plausible models for the accompanying instantaneous distributions. These can be applied to each point, and integrated over conversion to yield the complete composition and mass distributions at each point in conversion, including for the final product.

Here, we consider the bivariate distribution proposed by Stockmayer.[5] He proposed that when the monomer feed composition and the mean molecular weight and composition of the fraction polymerized are known, both the composition and chain length distributions can be obtained. In his theoretical model, the weight fraction of the part, with chain length L and composition deviation $u = (\Phi_A - F_A)$, $w(L,u)$ is given by

$$w(L,u)\,dL\,du = [\exp(-L/l^*)(1 - \beta_{com} + \beta_{com}L/l^*)L\,dL/L^{*2}][\sqrt{l/2\pi F_A F_B Q}] \times \exp(-Lu^2/2F_A F_B Q)\,du \quad (53)$$

where

$$Q = (1 - 4F_A F_B(1 - r_A r_B))^{1/2} \quad (54)$$

Φ_A is the molar fraction of A monomer units in a chain and β_{com} is the fraction of chains terminating by combination. The variable l is the length of a chain in monomer units, l^* is the number-average length of live radical chains. When β_{com} is 0, l^* is $(M_{w,inst}/m_{mon})/2$ and when it is 1, l^* is $(M_{w,inst}/m_{mon})/3$. For the general case, it can be written as

$$l^* = \frac{(4 - \beta_{com})}{(8 + \beta_{com})}\frac{M_{w,inst}}{m_{mon}} \quad (55)$$

Here $(M_{w,inst}/m_{mon})$ is the ratio of the M_w of the fraction polymerized at a specific instant to the average molecular weight of the comonomers, m_{mon}.

In an actual polymerization reaction, all concentrations are functions of time or, equivalently, of the degree of conversion. For this reason, Stockmayer's formula is valid only for the instantaneous values during a reaction. To find the bivariate distribution of the resulting polymer, Stockmayer's w function must be integrated over the conversion.

Results and Discussion

Figure 2 shows raw data for a typical experiment (experiment IV in Tables 1 and 2). The decrease in the UV shows principally the conversion of Sty, whereas the increase in the RI is due chiefly to the conversion of MMA. These two signals yield the concentrations of the comonomers, the polymer, and the monomer conversions, according to the expressions above. The monotonic increases of both the light scattering and viscosity also show the effect of an increasing concentration of polymer. The temperature of the reaction is also shown in the graph over the principal one. The average was 64.8 °C with an rms temperature fluctuation of 0.29 °C.

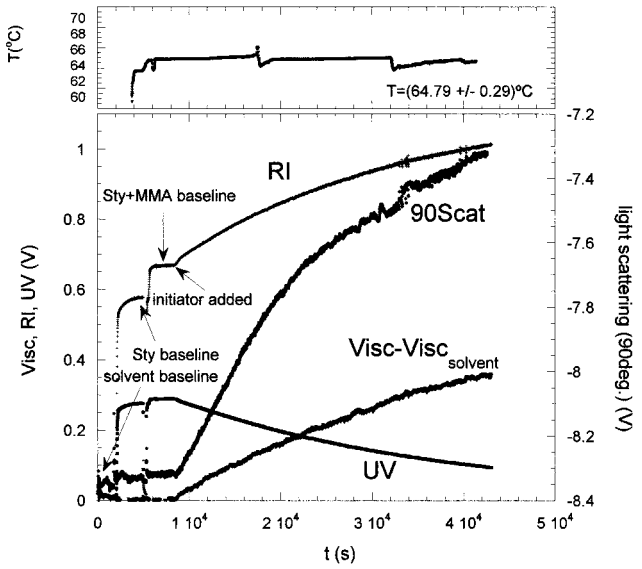

Figure 2. Raw data for UV, LS, RI, and viscometer detectors during a typical experiment (IV). The overset shows the temperature profile during the reaction.

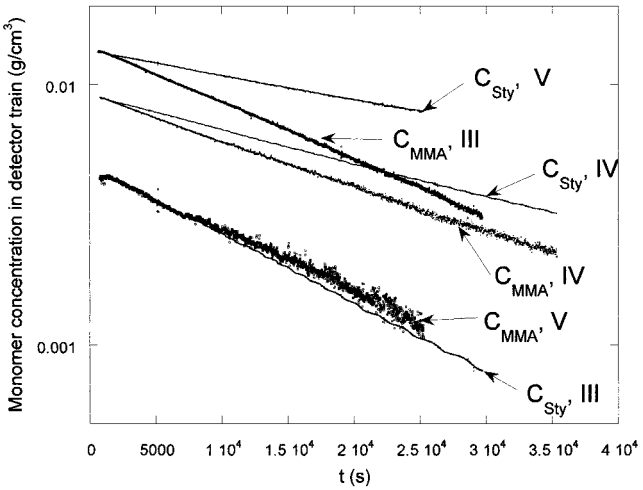

Figure 3. Concentrations in the detector train of Sty and MMA for several experiments (III, IV, and V in Table 1). The monomer decays are very well described by first-order fits, whose rate constants appear in Table 2. Data for a repeat of experiment V is also shown.

Figure 3 shows concentrations of each monomer for several experiments, as computed from the raw data, such as those of Figure 2, via eqs 1−7. The monomer decay in each case actually follows first-order kinetics over virtually the entire range of the experiment, as can be seen from the straight lines on the semilog plot representation. This indicates that the use of the approximations of steady state and slowly changing monomer concentration ratios are good ones. Final monomer conversion, p, ran from 50% to 70% in the experiments, due to reasons explained above.

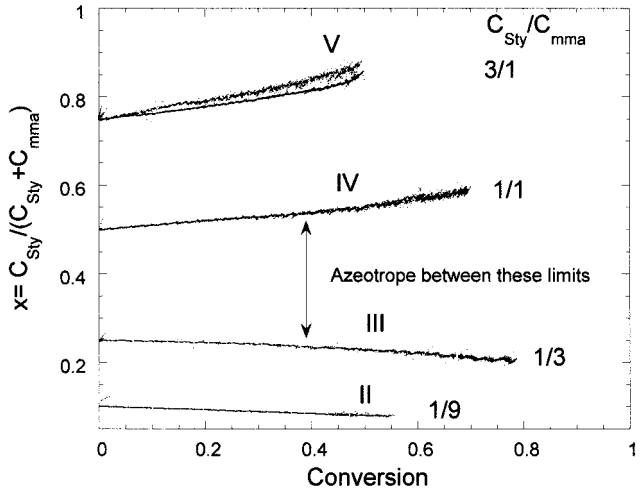

Figure 4. Evolution of styrene monomer fraction vs total monomer conversion p. From this, it is clear that the azeotropic point is between Sty/MMA = 1/1 to 1/3, that $1 > r_{MMA} > r_{Sty}$, and that the composition drift is not very significant in these experiments.

Monomer decay rates, final conversion, M_w, $[\eta]$, and final weight-average sequence length values are given in Table 2. Also shown are SEC results for M_w and polydispersity indices M_z/M_w and M_w/M_n. The values appear somewhere between the 3:2:1 ratios for M_z:M_w:M_n expected for termination by disproportionation and 4:3:2 ratios expected for termination by recombination.

O'Driscoll and co-workers have done considerable work on copolymerization kinetics and their conclusion is that while the Mayo–Lewis equation is often adequate for determining composition it fails to account for the kinetics. That failure to account for the kinetics was noted by other authors and resulted in the cross termination constant ϕ. This was attributed to penultimate effects rather than to termination effects. Two more reactivity speed ratios s_1 and s_2 were introduced to account for this. If the kinetic data from Table 1 are plotted (not shown), there is also deviation from Mayo–Lewis kinetics, as far as polymerization rate as a function of initial feed composition is concerned.

Figure 4 shows the evolution of styrene monomer fraction (x according to eq 15) vs total monomer conversion p. When the initial styrene fraction is 50% and 75% it increases throughout the reaction and when the initial fraction is 25% and 10% it monotonically decreases. This behavior is typical of systems with both reactivity ratios less than 1. Here it is clear that the azeotropic point is between a 1/1 and a 1/3 styrene to MMA ratio. This indicates that $1 > r_{MMA} > r_{Sty}$. We also see from the figure that the composition drift is not very significant in these experiments. This justifies the use of rate constants in estimating the reactivity ratios, below. Also shown in Figure 4 is a repeat of experiment V, showing good reproducibility.

Use of Initial Monomer Decay Rates To Determine r_A and r_B. If the composition drift and initiator decomposition rate are slow, the concentrations of A* and B* can be assumed almost constant throughout the reaction, so that [A] and [B], at least at early values of conversion, will yield first-order decay kinetics of the form

$$[A] = [A]_0 e^{-\alpha_A t} \quad \text{and} \quad [B] = [B]_0 e^{-\alpha_B t} \tag{56}$$

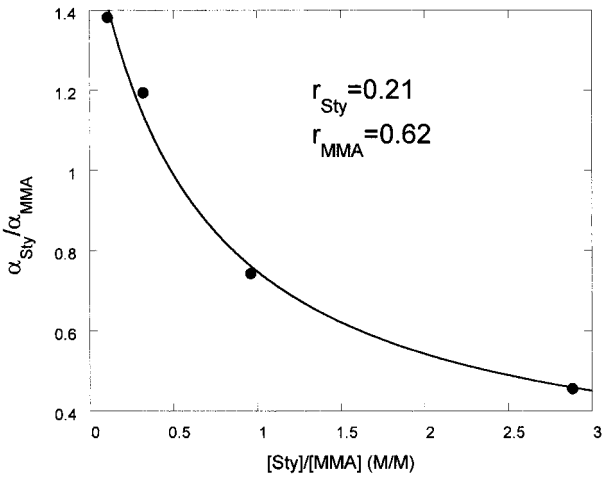

Figure 5. Determination of r_{Sty} and r_{MMA} using the ratio of Sty and MMA rate constants from eq 59. The values of r_{Sty} and r_{MMA} are 0.21 and 0.62, respectively.

where

$$\alpha_A = k_{AA}[A^*] + k_{BA}[B^*] \tag{57}$$

$$\alpha_B = k_{BB}[B^*] + k_{AB}[A^*] \tag{58}$$

Then, the reactivity ratios can be determined by finding the ratio of these rate constants, determined over early conversion, for two separate experiments in which the relative initial concentrations $[A]_0$ and $[B]_0$ are changed. That is, using eqs 9a,b with the steady-state assumption yields

$$\frac{\alpha_A}{\alpha_B} = \frac{1 + r_A\dfrac{[A]_0}{[B]_0}}{\dfrac{[A]_0}{[B]_0} + r_B} \tag{59}$$

Relative insensitivity of the right side of this equation to composition drift has been noted by Walling and Briggs,[60] and Kelen and Tudos have used this fact in developing their extended method.[61]

Figure 5 shows the determination of r_{Sty} and r_{MMA} using the ratio of Sty and MMA rate constants from eq 59. The values of r_{Sty} and r_{MMA} are 0.21 and 0.62, respectively. Even in the case of high drift, the initial decay rates—i.e., the initial slopes of semilog plots of monomer concentration vs time—should still yield a good approximation for the reactivity ratios.

Parts a–c of Figure 6 show the χ^2 contours of the EVM analysis obtained by comparing the monitored monomer depletion with the copolymerization equation as described in the section "Reactivity Ratios from Online Data."

Figure 6a shows the χ^2 contours for the statistically acceptable parts of the parameter space for the four experiments. The r(Sty) and r(MMA) axes are the reactivity ratios for Sty and MMA, respectively. The χ^2 contours are plotted only for ($\chi^2 < \chi^2_{best} + 30$) for clarity. Each experiment gives a long narrow valley as its region of confidence. The valleys are in the clockwise direction (from the steepest), for the experiments with 75%, 50%, 25%, and 10% Sty. The acceptable regions of each experiment intersect in the same area. Note that the regions of confidence corresponding to the acceptable

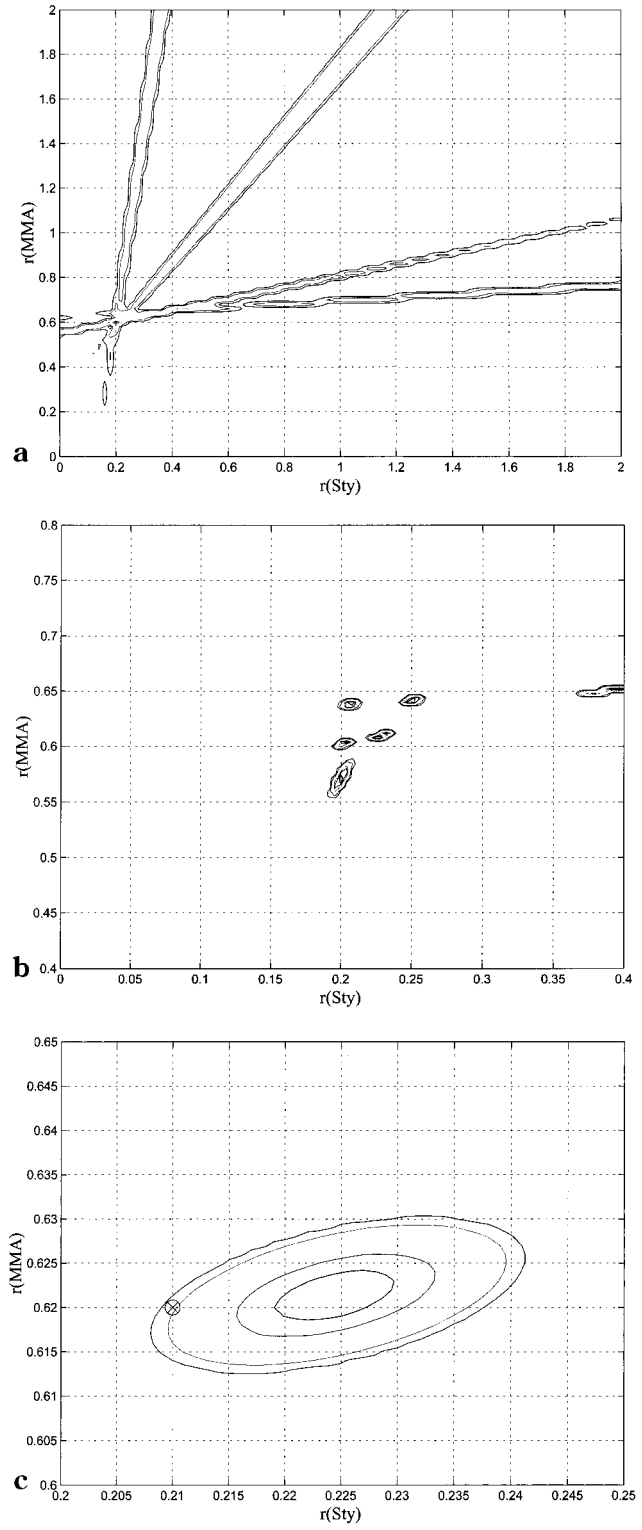

Figure 6. (a) χ^2 contours from the parameter space searches for the individual experiments: in clockwise order, starting from the steepest, V, IV, III, and II. (b) χ^2 contours for combined data for experiment pairs. (c) χ^2 joint confidence contours for the data in all four experiments (II, III, IV, V). The crossed circle represents r_{Sty} and r_{MMA} from the kinetic approach (Figure 5).

regions of experiments with 25% and 10% Sty are almost parallel.

In Figure 6b, the best fit values given by pairs of experiments are plotted. Five of the regions are closely packed, and the only outlying region is the long and narrow one for the joint confidence interval of the experiment pair with close initial compositions of 25% and 10% Sty. The five experiment pairs with widely differing initial compositions give small confidence regions and they are closely grouped. This close grouping indirectly validates the terminal model assumption in this work.

Figure 6c shows the joint confidence intervals for all four experiments. Each contour corresponds to one standard deviation. The best fit values $r_{Sty} = 0.225 \pm 0.01$ and $r_{MMA} = 0.621 \pm 0.01$ are very close to the $r_{Sty} = 0.21$ and $r_{MMA} = 0.62$ (shown by the crossed circle in Figure 6c) values, given by the approximate method based on monomer depletion rates.

While the method of using rate constants is convenient and follows immediately from the online data, the parameter search method is more rigorous, accounts quantitatively for error in the data, and, perhaps most significantly, applies to time-independent data. Hence, in principle, the polymerization reactions at a given temperature and starting ratios of monomer can be run at arbitrary and different concentrations of initiator and still be used for determining the reactivity ratios, whereas in the rate constant method of Figure 5 the same initiator concentration must be used in each experiment. The termination reaction and the cross-termination ratio effects can influence the simpler rate constant method but not the time-independent EVM.

Table 3 shows a compilation of reactivity ratios for a variety of solvents and initiator conditions.

Table 3. Reactivity Ratios for MMA/Sty from the Literature and This Work

solvent	*r*(Sty)	*r*(MMA)
dioxane[65]	0.56	0.53
acetone[65]	0.49	0.49
DMF[65]	0.38	0.45
cyclohexane[66]	0.35	0.56
cyclohexanone[66]	0.38	0.57
toluene[67]	0.534	0.393
bulk[68]	0.523	0.46
bulk UV irradiated[69]	0.39	0.22
bulk[70]	0.472	0.454
bulk[71]	0.5	0.5
bulk[71]	0.37	0.61
bulk[71]	0.57	0.41
bulk[71]	0.275	0.314
butyl acetate[a]	0.225	0.621

[a] This work.

Figure 7 shows $z(p)$ and $y(p)$, for the 1/1 reaction (IV in Table 1). $y(p)$ is computed directly from the monomer concentrations for Sty and MMA, whereas $z(p)$ is computed directly from the first-order fits to the monomer concentrations, which can be obtained from Figure 3. Direct differentiation of the monomer concentration data to obtain $z(p)$ leads to considerable noise.

Figure 8a shows the average composition distributions for each experiment. Using the expressions for the experimentally found first-order decays of MMA and Sty allows the copolymer composition distribution $\partial p/\partial z$ to be found analytically. These are shown, normalized to total polymer concentration in the detector, in Figure 8a. Because r_{Sty} and r_{MMA} are not widely different from each other, the compositional drift in the experiments is relatively small. As expected, the experiment closest to the azeotropic line gives the narrowest distribution.

Figure 8b shows the curves from Figure 8a integrated at each point with the Stockmayer distribution function given in eq 53.

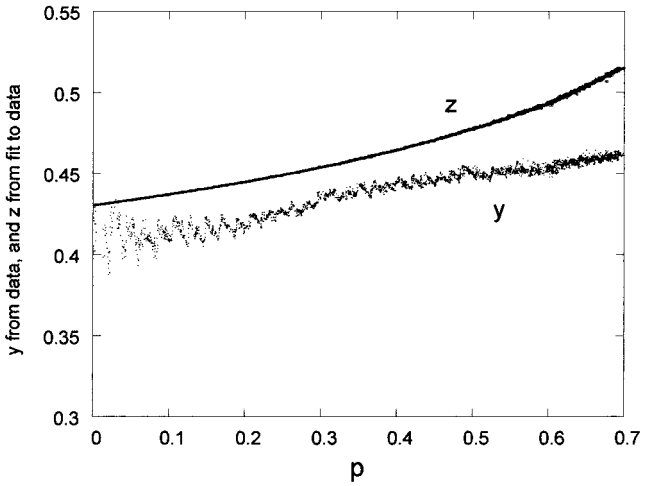

Figure 7. $z(p)$ and $y(p)$, for the 1/1 reaction. $y(p)$ is computed directly from the monomer concentrations for Sty and MMA, whereas $z(p)$ is computed directly from the first-order fits to the monomer concentrations, which can be obtained from Figure 3.

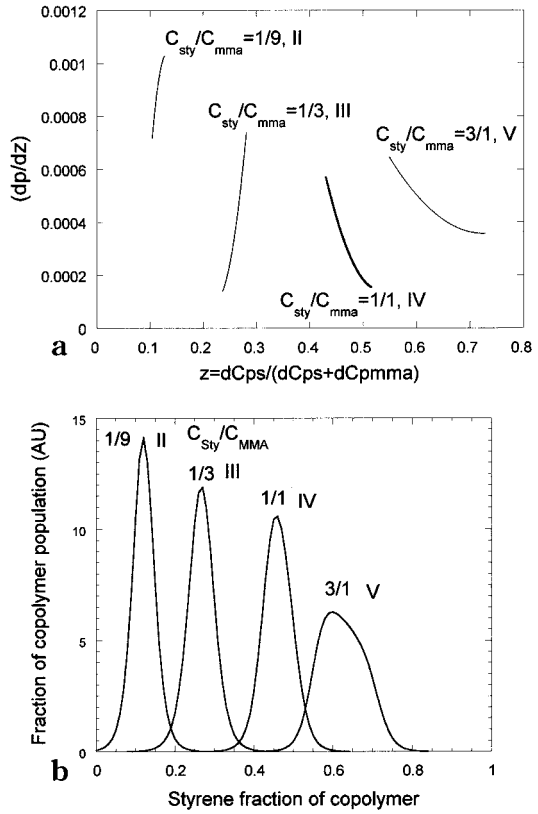

Figure 8. (a) Normalized composition distributions. As expected, the experiment closest to the azeotropic line gives the narrowest distribution. (b) Composition distribution curves obtained from Figure 8a integrated at each point over the composition portion of the Stockmayer distribution function given in eq 60.

Figure 9a shows the instantaneous number and weight-average Sty sequence lengths, $\langle N_{\mathrm{Sty}}\rangle_{\mathrm{n}}$ and $\langle N_{\mathrm{Sty}}\rangle_{\mathrm{w}}$, respectively, vs conversion, for experiment V. These values are computed from eqs 19−21, using the best value of $r_{\mathrm{Sty}} = 0.225$. The cumulative averages are shown in the figure to be $\langle N_{\mathrm{Sty}}\rangle_{\mathrm{n,cumu}} = 2.21$ and $\langle N_{\mathrm{Sty}}\rangle_{\mathrm{w,cumu}} = 3.40$. The inset to the figure shows the actual instantaneous Sty sequence length distributions, $P_{\mathrm{Sty},k}$, obtained when the conversion was equal to 0, 0.3, and 0.5.

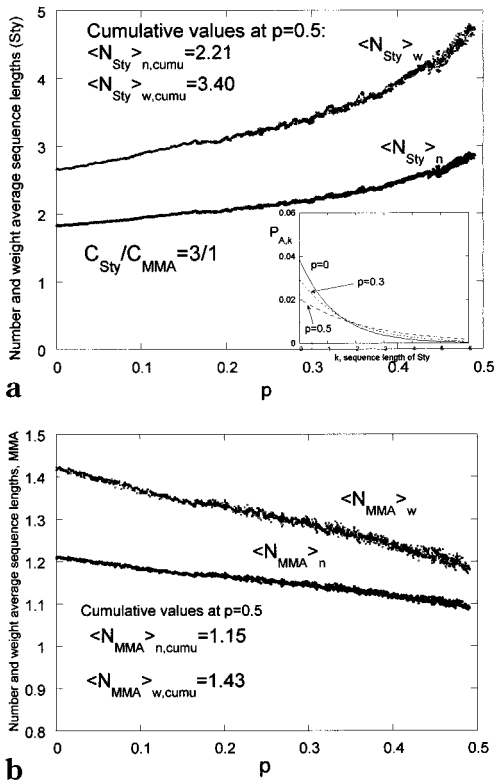

Figure 9. (a) Instantaneous number and weight-average sequence lengths for Sty vs conversion for experiment V. The inset shows the instantaneous sequence length distributions according to eqs 18 and 19 for selected conversion points 0, 0.3, and 0.5. (b) Same as part a, except for MMA.

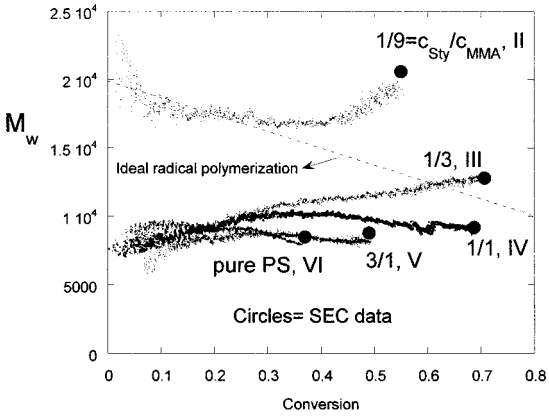

Figure 10. M_{w} vs total monomer conversion, p, from the light-scattering data. The circles show SEC results for the end product of each reaction.

Figure 9b shows the instantaneous number and weight-average MMA sequence lengths. The values were computed from eqs 19−21, substituting B (MMA) subscripts for all A subscripted variables, and using the best fit value, $r_{\mathrm{MMA}} = 0.621$. Table 2 gives the cumulative values of the weight-average sequence length for Sty, $\langle N_{\mathrm{Sty}}\rangle_{\mathrm{w,cum}}$, integrated over the entire conversion range, according to eq 22, and similarly for MMA.

Figure 10 shows M_{w} vs total monomer conversion, p. The value of $K'c_{\mathrm{p}}/I(c_{\mathrm{p}} = 0, q = 0)$ was required to find M_{ap}, whence M_{w} was computed for each conversion point. The multiangle light-scattering detector gave no angular dependence to the light-scattering data, so it sufficed in the analysis to use just the scattering data from $\theta = 90°$. The light-scattering procedure developed

above was applied to the ACOMP data. Namely, $z(p)^2$ was fit to a polynomial of 3rd order, and eq 49 was applied in order to arrive at the ratio M_{ap}/M_w. Because of the quasi-azeotropy of the reactions, the light-scattering correction factor due to compositional heterogeneity never exceeded 2%.

Since the measurements were made at small, but finite concentration, however, there was a small correction due to the A_2 effect included in the data of Figure 10. Table 2 shows that A_2 varies monotonically between its value for pure PMMA (0.00013) and pure PS (0.00045) as the fractional content of Sty increases in the copolymer. The values of A_2 in the table were found from continuous dilution experiments performed on the endproducts of each of the reactions.

In principle, the complex average of A_2 found by light scattering, which involves variable excluded volume interactions for both a polydisperse population, as detailed by Cassassa[62] and others,[63] and a chemically heterogeneous population could be built from the knowledge of both composition and mass obtained in ACOMP, as first treated by Stockmayer, Fixman, and Epstein.[40] Because the A_2 correction in these experiments is small, and composition drift minimal, the correction was made simply by using the A_2 values from Table 2 obtained from separate experiments on the endproducts.

The fractional error introduced by an uncertainty of ΔA_2 leads to an uncertainty in M_w given by

$$\frac{\Delta M_w}{M_w} = 2\Delta A_2 M_w c_p \tag{60}$$

where c_p is the polymer concentration in the detector. Under the conditions of the current experiments the quantity $2A_2c_pM_w$ is itself generally well below 10%, and further error introduced by ΔA_2 from varying composition will be much smaller than this. In general, it is possible to arrange ACOMP conditions so that A_2 effects are negligible, or at least minimized.

The circles in Figure 10 show that the SEC values obtained on the reaction endproducts are virtually identical to the ACOMP results.

Interestingly, M_w does not change significantly during conversion in any of the experiments, except III, where there is a measurable increase in M_w. For this reason we do not proceed to compute mass distributions based on $M_{w,inst}$. For ideal radical polymerization in the absence of chain transfer, due to decreasing monomer to initiator concentration ratio, M_w should decrease linearly with conversion according to

$$M_w(f) = M_w(0)\left[1 - \frac{f}{2}\right] \tag{61}$$

and the instantaneous value decreases as

$$M_{w,inst}(f) = M_w(0)[1 - f] \tag{62}$$

There are two immediate possibilities for the near constancy of $M_w(f)$: (1) chain transfer to monomer and (2) decreasing initiator concentration. For conceptual simplicity, consider the homopolymeric case. In the case of chain transfer to an agent S, the reaction

$$R + S \xrightarrow{k_3} S^* + P$$

applies, where R is the propagating macroradical and P is the dead polymer chain. S* can subsequently transfer to monomer to initiate a new chain, with rate constant k_4. When $k_3 < k_4$, the initial transfer to R is rate controlling, and it is well-known (e.g., ref 57) that the instantaneous number-average degree of polymerization $N_{n,inst}$ is given by

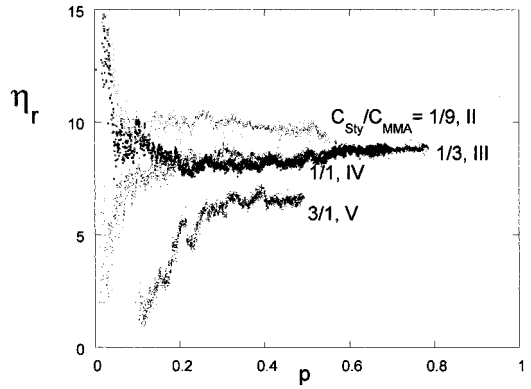

Figure 11. Reduced viscosity (cm^3/g) vs conversion. The trends are similar to those for M_w: i.e., no strong change during the reactions, and both terminal viscosity and M_w decrease as the initial fraction of Sty increases.

$$N_{n,inst} = \frac{k_p[m]}{Yk_t[R] + k_3[S]} \tag{63}$$

where $Y = 1$ for termination by recombination and $Y = 2$ for termination by disproportionation. Hence, if the transfer agent is the monomer itself, and $k_3[m] \gg Yk_t[R]$, then $N_{n,inst}$ will remain constant.

Under the second possibility, if the initiator decay rate is faster than or comparable to the conversion rate, then [R] will decrease. If [R] decreases at a rate comparable to the decrease in [m], then $N_{n,inst}$ can also remain constant, even in the absence of any chain transfer. In this case, however, [m](t) would show a "stretched exponential" decay.[64] The decays in Figure 2 appear too well fit by a simple exponential to fit with this argument. A similar constancy in M_w vs conversion was also found in ref 31, although no definitive reason for it was found.

Figure 11 shows viscosity vs conversion and the trends are similar to those for M_w; i.e., no strong change during the reactions, and both terminal viscosity and M_w decrease as the initial fraction of Sty increases. The viscosity measurements provide a good cross-check on the light-scattering measurements insofar as they require no correction factors. On the other hand they do not directly furnish M_w. The magnitudes of the viscosity are such that the ACOMP measurements were made far below the overlap concentration threshold, which is roughly the reciprocal of [η]: i.e., on the order of 0.1 g/cm^3. Viscosities were measured at more than 10 times less than this value, so that the reduced viscosities should be very close to [η]. An early treatment of how [η] varies with copolymerization was given by Stockmayer et al.[40]

Figure 12 shows raw SEC chromatograms for the final products of both the copolymer and homopolymer reactions. In SEC higher masses elute at lower elution volumes, so that these chromatograms confirm the trends revealed by M_w and viscosity, that average mass decreases as the fraction of initial Sty increases. Table 1 shows the SEC values of M_w and [η], which are in excellent agreement with the ACOMP values. Addition-

Table 4. Model Independence and Dependence of the Copolymer Characteristics Determined by ACOMP

copolymer characteristic	model dependence
av instantaneous composition	none
av composition distribution	none
cumulative av M_w	none
instantaneous av M_w	none
av cumulative mass distribution	none
instantaneous av sequence length	Mayo−Lewis equation
cumulative av sequence length	Mayo−Lewis equation
instantaneous sequence length distribution	Mayo−Lewis equation
cumulative sequence length distribution	Mayo−Lewis equation
instantaneous molecular mass distribution	Stockmayer/Flory
cumulative molecular mass distribution	Stockmayer/Flory
inst. composition distribution	Stockmayer/Mayo−Lewis
composition distribution	Stockmayer/Mayo−Lewis
reactivity ratios	Mayo−Lewis

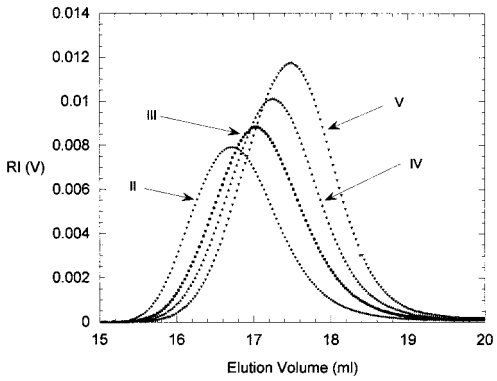

Figure 12. Raw SEC RI chromatograms for the final products of both the copolymer and homopolymer reactions.

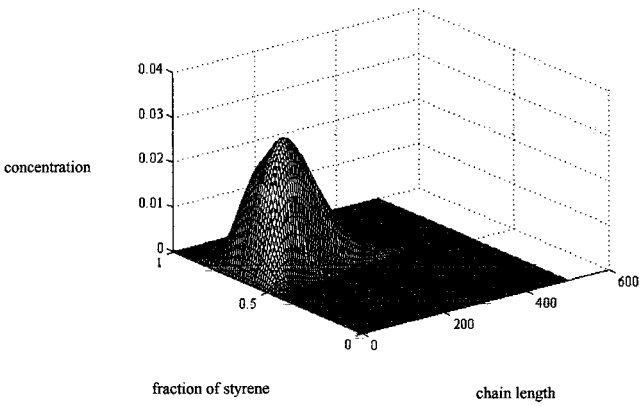

Figure 13. 3-D bivariate distribution for experiment V, using the Stockmayer bivariate distribution (eq 53).

ally, SEC provides the polydispersity indices, M_w/M_n and M_z/M_w, which are also shown in Table 2.

With the M_w and composition data available, the procedure outline above for computing the Stockmayer bivariate distribution was applied. An example of this is shown in Figure 13, for which the procedure was applied to the results of experiment V.

Summary

ACOMP instrumentation, procedures, and analyses have been adapted to monitoring free radical copolymerization reactions. The differences in comonomer and copolymer values of UV absorption and differential refractive index increments make it possible to obtain a continuous record of comonomer and copolymer concentrations.

From this, model-independent average instantaneous and cumulative composition distributions were computed. Use of simultaneous light-scattering data, together with the detailed composition data mean that, not only can the traditional method of making scattering measurements in three different solvents be avoided, but the evolution of M_w can be followed, again, in model-independent fashion. Derivative techniques can also be used to follow the evolution of the polydispersity of the copolymer population, but were not applied here since M_w was fairly constant throughout each reaction.

Well-accepted model-dependent assumptions about the nature of instantaneous composition and mass distributions allow the average data to be integrated to produce realistic representations of the full bivariate distribution. Further use of the differential viscometer yields both valuable information on the copolymer intrinsic viscosity and a cross-check on the masses derived from light-scattering behavior.

Reactivity ratios were computed using two distinct methods; initial kinetics, and a parameter space search. Furthermore, it is possible to determine the instantaneous and cumulative sequence length distributions and averages, based on the Mayo−Lewis model. In further work, combining the viscosity and light-scattering may provide information on branching. Deductions about kinetics and mechanisms can also be made from these combined measurements.

Table 4 summarizes which copolymer characteristics are model independent and which are model dependent.

Since the reactivity ratios of MMA and Sty are not widely different, there were not large composition drifts during the reactions. Hence, future work involving comonomers with widely different reactivity ratios could be used to assess the robustness of the entire technique for both broad composition and mass distributions.

Extending ACOMP to graft and block copolymerization should be possible, although there will certainly be both experimental and computational problems to resolve statistical and block copolymerization using "living" techniques, such as controlled radical polymerization and atom transfer radical polymerization, should provide fertile extension of ACOMP.

Finally, it is hoped that ACOMP for copolymerization will ultimately prove useful in controlling the quality of copolymers during industrial scale production.

Acknowledgment. Support from NSF CTS 0124006, NSF INT-0080624, and TUBITAK−NSF TBAG-U/2(100T14) for US/Turkey collaboration are acknowledged. A.G. acknowledges support from İ.T.Ü. Geliştirme Vakfı and İ.T.Ü. Research Fund. We thank A. Kargol of Tulane and O. Özcan of İ.T.Ü. for help with the Matlab figures.

Glossary of Terms

A	monomer A (and likewise for B)
A*	propagating radical A
[A]	molar concentration of monomer A
[A*]	molar concentration of propagating radical A
A_2	second virial coefficient
c_{mA}	mass concentration of monomer A
c_{pA}	mass concentration of A in polymeric form
c_p	total mass concentration of copolymer
f_A	mole fraction of A left in solution (eq 16)
F_A	instantaneous mole fraction of A incorporated into copolymer (eq 12)
$I(q,c_p)$	total copolymer solution excess Rayleigh scattering minus that of the solvent (eq 23)
k_{AA}	propagation rate for A adding to A*
k_{AB}	propagation rate for B adding to A*
k_p	second-order viscosity constant (eq 8)
K'	light scattering optical constant (eq 29)
l	length of a chain in monomer units
l^*	number-average length of live radical chains (eq 55)
m_{mon}	average monomer mass of the comonomers
M_A	cumulative weight-average of A portion of polymer (eq 35)
M_{ap}	mass obtained from $K'\nu^2 c_p I(q=0,c_p=0)$ without taking into account the compositional heterogeneity of the copolymer sample (eqs 32, 33)
M_w	cumulative weight-average molecular weight (eq 37)
$M_{w,inst}$	instantaneous weight-average molecular weight (eq 41)
N_A	Avogadro's number
$\langle N_A\rangle_n$	instantaneous number-average sequence length of A (eq 20)
$\langle N_A\rangle_w$	instantaneous weight-average sequence length of A (eq 21)
$\langle N_A\rangle_{n,cum}$	cumulative number-average sequence length of A (eq 22)
$\langle N_A\rangle_{w,cum}$	cumulative weight-average sequence length of A (eq 22)
p	total monomer mass conversion (eq 16)
p_A	conversion of monomer A
$P_{A,k}$	sequence length distribution: probability of occurrence of a sequence of k monomers of type A, terminated by a monomer of type B
q	scattering vector amplitude (eq 24)
r_A	reactivity ratio of A (eq 11)
R_A	initial volume of monomer A/solvent volume, in the reactor.
$\langle S^2\rangle_z$	z-average mean square radius of gyration
u	composition deviation
$w(l,u)$	weight fraction of polymers of degree of polymerization of l and composition deviation u (eq 53)
W_{AA}	probability that A* adds to A (eq 22)
x	average mass fraction of monomer A left in solution (eq 15)
y	average mass fraction of A in copolymer form (eq 31)
z	instantaneous fraction of A incorporated into copolymer (eq 17)
α_A	first-order decay constant of A
β_{com}	the fraction of chains terminating by combination
δ_A	$1 - \rho_{mA}/\rho_{pA}$
$[\eta]$	weight-average intrinsic viscosity
η_r	weight-average reduced viscosity
Φ_A	fraction of A monomer units in a particular chain
λ	laser vacuum wavelength
ν	differential index of refraction of the copolymer solution is a given solvent (eqs 26, 30)
ν_A	differential index of refraction of homopolymer A in a given solvent
ρ_{mA}	density of monomer A
ρ_{pA}	density of polymer A
θ	light scattering measurement angle
χ^2	mean square deviation between data and data fit (eq 14)

References and Notes

(1) Mayo, F. R.; Lewis, F. M. *J. Am. Chem. Soc.* **1944**, *66*, 1594−1601.
(2) Alfrey, T.; Goldfinger, G. *J. Chem. Phys.* **1944**, *12*, 205−209.
(3) Wall, F. T. *J. Chem. Phys.* **1945**, *13*, 1929−1931.
(4) Simha, R.; Branson, H. *J. Chem. Phys.* **1944**, *12*, 253−267.
(5) Stockmayer, W. H. *J. Chem. Phys.*, **1945**, *13*, 199−207.
(6) Tobita, H. *Polymer* **1998**, *39*, 2367−2372.
(7) Duc, S.; Petit, A. *Polymer* **1999**, *40*, 589−597.
(8) Dammert, R.; Jussila, M.; Vastamaki, P.; Riekkola, M.-L.; Sundholm, F. *Polymer* **1997**, *38*, 6273−6280.
(9) Feng, Y.; Hay, J. N. *Polymer* **1998**, *39*, 6723−6731.
(10) Xu, J.; Feng, L. *Eur. Polym. J.* **2000**, *36*, 867−878.
(11) Wignall, G. D.; Alamo, R. G.; Ritchson, E. J.; Mandelkern, L.; Schwahn, D. *Macromolecules* **2001**, *34*, 8160−8165.
(12) Faldi, A.; Soares, J. B. P. *Polymer* **2001**, *42*, 3057−3066.
(13) Cools, P. J. C.; Maesen, F.; Klumperman, B.; van Herk, A. M.; German, A. L. *J. Chromatogr. A* **1996**, *736*, 125−130.
(14) Verhelst, V.; Vandereecken, P. *J. Chromatogr. A* **2000**, *87*, 269−277.
(15) Schunk, T. C.; Long, T. E. *J. Chromatogr. A* **1995**, *692*, 221−232.
(16) Kikuchi, A.; Nose, T. *Polymer* **1995**, *36*, 2781−2786.
(17) Yau, W. W.; Gillespie, D. *Polymer* **2001**, *42*, 8947−8958.
(18) Tsai, C. H. Y.; Thomas, E. L.; MacKnight, W. J.; Schneider, N. S. *Polymer* **1986**, *27*, 659−666.
(19) Suen, W.; Kaltashov, I.; Hsu, S. L *Polym. Mater. Sci. Eng.* **2000**, 82 363−364.
(20) Suzuki, H.; Nishio, Y.; Kimura, N.; Mathot, V. B. F.; Pijpers, M. F. J.; Murakami, Y. *Polymer* **1994**, *35*, 3698−3702.
(21) Haftka, S.; Koennecke, K. J. *Macromol. Sci., Phys.* **1991**, *B30*, 319−334.
(22) Avella, M.; Greco, P.; Malinconico, M. *Int. J. Polym. Mater.* **1988**, *12*, 147−164.
(23) Bera, P.; Saha, S. K. *Eur. Polym. J.* **2000**, *36*, 411−419.
(24) Starck, P.; Lofgren, B. *Eur. Polym. J.* **2002**, *38*, 97−107.
(25) Curtis, M. D. *Macromolecules* **2001**, *34*, 7905−7910.
(26) Witt, U.; Mueller, R.-J.; Deckwer, W.-D. *Macromol. Chem. Phys.* **1996**, *197*, 1525−1535.
(27) Thorn-Csanyi, E.; Perner, H. *Makromol. Chem.* **1979**, *180*, 919−928.
(28) Tanaka, Y.; Sato, H.; Nakafutami, Y. *Polymer* **1981**, *22*, 1721−1723.
(29) Kakuta, K.; Tamai, H.; Wong, P.-H.; Kawahara, S.; Tanaka, Y. *Macromolecules* **1999**, *32*, 5994−5997.
(30) Barreiro, M. F.; Dias, R. C. S.; Costa, M. R. N. *Macromolecules* **1994**, *27*, 7650−7653.
(31) Florenzano, F. H.; Strelitzki, R.; Reed, W. F. *Macromolecules* **1998**, 7226−7238.
(32) Grassl, B.; Reed, W. F. *Macromol. Chem. Phys.* **2002**, *203*, 586−597.
(33) Giz, A.; Giz, H.; Brousseau, J.-L.; Alb, A. M.; Reed, W. F. *Macromolecules* **2001**, *34*, 1180−1191.
(34) Grassl, B.; Alb, A. M.; Reed, W. F. *Macromolecular Chem. Phys.* **2001**, *12*, 2518−2524.
(35) Reed, W. F. *Macromolecules* **2000**, *33*, 7165−7172.
(36) Chauvin, F.; Alb, A. M.; Bertin, D.; Tordo, P.; Reed, W. F. *Macromol. Chem. Phys.*, in press.
(37) Strelitzki, R.; Reed, W. F. *J. App. Polym. Sci.* **1999**, *73*, 2359−2368.
(38) Norwood, D. P.; Reed, W. F. *Int. J. Polym. Anal. Charact.* **1997**, *4*, 99−132.

(39) Brousseau, J.-L.; Giz, H. Ç.; Reed, W. F. *J. Appl. Polym. Sci.* **2000**, *77*, 3259−3262.
(40) Stockmayer, W. H.; Moore, L.D.; Fixman, M.; Epstein, B. N. *J. Polym. Sci.* **1955**, *16*, 517−530.
(41) Bushuk, W.; Benoit, H. *Can. J. Chem.* **1958**, *36*, 1616−1626.
(42) Huggins, M. L. *J. Am. Chem. Soc.* **1942**, *64*, 2716−2722.
(43) Sorci, G. A.; Reed, W. F. *Langmuir* **2002**, *18*, 353−364.
(44) Skeist, I. *J. Am. Chem. Soc.* **1946**, *68*, 1781−1784.
(45) Meyer, V. E.; Lowry, G. G. *J. Polym. Sci., Part A* **1965**, *3*, 2843−2851.
(46) Tidwell, P. W.; Mortimer, G. A. *J. Polym. Sci., Part A* **1965**, *3*, 369−387.
(47) McFarlane, R.; Reilly, P. M.; O'Driscoll, K. F. *J. Polym. Sci., Polym. Chem. Ed.* **1980**, *18*, 251−257.
(48) Patino-Leal, H.; Reilly, P. M.; O'Driscoll, K. F. *J. Polym. Sci., Polym. Lett. Ed.* **1980**, *18*, 219−227.
(49) Dube, M.; Sanayei, R. A.; Penlidis, A.; O'Driscoll, K. F.; Reilly, P. M. *J. Polym. Sci., Part A: Polym. Chem. Ed.* **1991**, *29*, 703−708.
(50) Van Herk, A. M. *J. Chem. Educ.* **1995**, *72*, 138−140.
(51) Van Herk, A. M.; Dröge, T. *Macromol. Theory Simul.* **1997**, *6*, 1263−1276.
(52) Giz, A. T. *Macromol. Theory Simul.* **1998**, *7*, 391−397.
(53) Van der Meer, R.; Linssen, H. N.; German, A. L. *J. Polym. Sci., Polym. Chem. Ed.* **1978**, *16*, 2915−2930.
(54) Chee, K. K.; Ng, S. C. *Macromolecules* **1986**, *19*, 2779−2787.
(55) Giz, A.; Catalgil-Giz, H.; Sunbul, D.; Reed, W. F. Submitted for publication.
(56) Press, W.; Flannery, B. P.; Tsilkovsky, S. A.; Vetterling, W. T. *Numerical Recipes*; Cambridge University Press: Cambridge, England, 1986.
(57) Rodriguez, F. *Principles of Polymer Systems*, 3rd ed; Hemisphere Pub. Corp.: Bristol, PA, 1989.
(58) Odian, G. *Principles of Polymerization*, 3rd ed; John Wiley & Sons: New York, 1991.
(59) Zimm, B. H. *J. Chem. Phys.* **1948**, *16*, 1093−1099.
(60) Walling, C. H.; Briggs, E. R. *J. Am. Chem. Soc.* **1945**, *67*, 1774−1778.
(61) Kelen, T.; Tudos, F.; Turksanyi, B.; Kennedy, J. P. *J. Polym. Sci., Polym. Chem. Ed.* **1977**, *15*, 3047−3074.
(62) Cassassa, E. F. *Polymer* **1962**, *3*, 625−631.
(63) Muthukumar, M.; Nickel, J. *J. Chem. Phys.* **1987**, *86*, 460−465.
(64) Dotson, N. A.; Galvan, R.; Laurence, R. L.; Tirrel, M. *Polymerization Process Modeling*; VCH Pub.: New York, 1996.
(65) Bonta, G.; Gallo, B. M.; Russo, S. *Polymer* **1975**, *16*, 429−432.
(66) Talpur, M. M. A.; Kaim, A.; Guttman, T. K.; Pirzada, T. *Arabian J. Sci. Eng.* **1999**, *24*, 133-140.
(67) Fukuda, T.; Kubo, K.; Ma, Y.-D.; Inagaki, H. *Polym. J.* **1987**, *19*, 523−530.
(68) Fukuda, T.; Ma, Y.-D.; Inagaki, H. *Macromolecules* **1985**, *18*, 17−26.
(69) Ramelow, Ü. S.; Qiu, Q. H. *J. Appl. Polym. Sci.* **1995**, *57*, 911−920.
(70) O'Driscoll, K. F.; Kale, L. T.; Rubio, L. H. G.; Reilly, P. M. *J. Polym. Sci.* **1984**, *22*, 2777−2788.
(71) Greenly, R. Z. In *Polymer Handbook*, 3rd ed; Brandrup, J.; Immergut, E. H., Grulke, A. E., Eds.; pII/234−235; Wiley: New York, 1999.

MA0201983